

Delayed ^{68}Ga -FAPi-46 PET/MR imaging confirms ongoing fibroblast activation in patients after acute myocardial infarction

Jana Kupusovic^{a,b,1,2}, Lukas Kessler^{c,1,2}, Sandra Kazek^{c,1}, Michal Kamil Chodyla^{d,1}, Lale Umutlu^{d,1}, Fadi Zarrad^{c,1}, Michael Nader^{c,1}, Wolfgang P. Fendler^{c,1}, Zohreh Varasteh^{c,e,1}, Ken Hermann^{c,1}, Dobromir Dobrev^{f,g,h,1}, Reza Wakili^{a,b,i,1}, Tienush Rassaf^{a,1}, Johannes Siebermair^{a,j,1,2}, Christoph Rischpler^{c,k,1,2,*}

^a Department of Cardiology and Vascular Medicine, West German Heart and Vascular Center Essen, University of Duisburg-Essen, Essen, Germany

^b Department of Medicine and Cardiology, Goethe University, Frankfurt, Germany

^c Department of Nuclear Medicine, University Hospital Essen, University of Duisburg-Essen, Essen, Germany

^d Department of Diagnostic and Interventional Radiology, University Hospital Essen, University of Duisburg-Essen, Essen, Germany

^e Department of Nuclear Medicine, Klinikum Rechts der Isar der TUM, Technical University of Munich, Munich, Germany

^f Institute of Pharmacology, West German Heart and Vascular Center, University Duisburg-Essen, Essen, Germany

^g Department of Molecular Physiology & Biophysics, Baylor College of Medicine, Houston, TX, United States

^h Department of Medicine and Research Center, Montreal Heart Institute and Université de Montréal, Montréal, Quebec, Canada

ⁱ German Center for Cardiovascular Research DZHK, Partner site Rhine-Main, Germany

^j Department of Cardiology, Krankenhaus Göttlicher Heiland GmbH, Vienna, Austria

^k Department of Nuclear Medicine, Klinikum Stuttgart, Stuttgart, Germany

ARTICLE INFO

Keywords:

FAPi
Fibroblast activation
Myocardial infarction
Acute coronary syndrome
Cardiovascular imaging
PET/MRI

ABSTRACT

Purpose of the Report: Combined cardiac ^{68}Ga -Fibroblast-Activation Protein-alpha inhibitor (FAPi) positron-emission tomography (PET) and cardiac magnetic resonance imaging (MRI) constitute a novel diagnostic tool in patients for the assessment of myocardial damage after an acute myocardial infarction (AMI). Purpose of this pilot study was to evaluate simultaneous Ga-68-FAPi-46-PET/MR imaging in the delayed phase after AMI.

Material and Methods: Eleven patients underwent hybrid ^{68}Ga -FAPi-46 PET/MRI post AMI. Standardized uptake values and fibroblast activation volume (FAV) were calculated and correlated with serum biomarkers and MRI parameters.

Results: Significant ^{68}Ga -FAPi-46 uptake could be demonstrated in 11 (100 %) patients after a mean period of 30.9 ± 22.0 days. FAV significantly exceeded the infarction size in MRI and showed a good correlation to MRI parameters as well as to serum biomarkers of myocardial damage.

Conclusions: ^{68}Ga -FAPi-46 PET/MRI offers molecular and morphological imaging of affected myocardium after AMI. This study demonstrates ongoing fibroblast activation in a delayed phase after AMI and generates hypotheses for future studies while aiming for a better understanding of myocardial remodeling following ischemic tissue damage.

1. Introduction

Activation of a pro-inflammatory phenotype in fibroblasts is a known phenomenon after tissue injury in a short-term period after myocardial ischemia [1]. The fibroblast activation protein (FAP) alpha has been shown to be an important contributor to this process, leading to

myocardial remodeling and to consecutive development of replacement fibrosis [1–3]. The latter aims at the stabilization of the myocardial architecture after injury and reflects an important healing mechanism following myocardial damage. Nonetheless, excessive fibrosis development has been suggested to impair ventricular function leading to the development of chronic heart failure and arrhythmias due to electrical

* Corresponding author at: Department of Nuclear Medicine, Klinikum Stuttgart, Stuttgart, Germany.

E-mail address: c.rischpler@klinikum-stuttgart.de (C. Rischpler).

¹ This author takes responsibility for all aspects of the reliability and freedom from bias of the data presented and their discussed interpretation.

² First and last authors contributed equally to the present work.

disparities [1,4,5]. The pathophysiology of ventricular fibrosis is incompletely understood, especially the timeline of fibrotic remodeling following ischemic injury [4]. Cardiac magnetic resonance imaging (MRI) with late gadolinium enhancement (LGE) is an established tool in the assessment of a persistent structural damage following acute myocardial infarction (AMI) [6]. With respect to functional imaging, positron-emission tomography (PET) imaging with radio-labeled FAP inhibitors (FAPI) offers the chance to assess FAP expression in-vivo as surrogate for fibroblast activation in post-ischemic myocardial tissue [7,8]. Imaging of the extent of fibroblast activation in an animal AMI model demonstrated a maximum FAPI-uptake at day 6 after ischemic injury, with the uptake decreasing rapidly within the following 2 weeks. The first PET studies in humans confirmed fibroblast activation early on after AMI and showed that the FAPI signal exceeded the LGE area on MRI [8,9].

While previous studies have shown the persistence of FAPI signal in the subacute phase of AMI up to 11 days [8], the aim of the present study was to investigate if FAPI uptake as surrogate for fibroblast activation persists in the delayed phase after myocardial ischemia, thereby suggesting ongoing fibrotic remodeling in humans after AMI. Further, the study aimed for an analysis if patients with non-ST elevation myocardial infarction [NSTEMI] showed different patterns of FAPI uptake compared to STEMI patients.

2. Methods

2.1. Patients

In this retrospective study, we analyzed a total of 11 patients after AMI and percutaneous coronary intervention, who underwent ^{68}Ga -FAPI-46 PET/MRI at 30.9 \pm 22 days after AMI. All patients gave written informed consent to undergo clinical ^{68}Ga -FAPI-46 PET/MRI following the regulations of the German Pharmaceuticals Act §13(2b). Retrospective analysis of PET/MRI and clinical data was approved by the local ethics committee for the purpose of the present study (permit no. 20-9777-BO) and requirement to obtain study-specific informed consent was waived. This study was performed on a dedicated hybrid PET/MRI scanner in order to simultaneously assess FAPI/PET and established MRI data of myocardial damage. Further, clinical and serum biomarkers were assessed.

2.2. Radiotracer synthesis and image acquisition

The synthesis of ^{68}Ga -FAPI-46 was performed as previously described [7]. Scans were performed on a dedicated 3 Tesla PET/MRI system (Biograph mMR; Siemens, Erlangen, Germany) using standard acquisition and reconstruction protocols (detailed in the supplemental methods). Injected activity of ^{68}Ga -FAPI-46 was 126.9 \pm 49.8 MBq. Acquisition of PET data of the thorax were performed 10 min p.i. over 20 min. PET images were iteratively reconstructed (4 iterations, 5 subsets, matrix: 220 \times 220, Gauss filtering: 5 mm) taking into account time-of-flight information, using dedicated manufacturer's software (syngo MI.PET/CT; Siemens Healthineers).

2.3. Cardiac magnetic resonance imaging

Global analysis included assessment of left ventricular ejection fraction (LVEF) as well as the area of myocardial injury estimated by LGE.

2.4. Image evaluation

Images were interpreted by two nuclear medicine specialists and radiologists for PET and MRI based on a consensus decision (LK and CR). In case of discordance a third specialist (WPF) was consulted. Standardized uptake values (SUV_{max} , SUV_{peak} , SUV_{mean}) and fibroblast

activation volume (FAV) were measured with a region grow algorithm with a threshold of 50 % of the maximum uptake in the infarcted myocardium. Tracer uptake in non-infarcted remote myocardium or in blood pool (right atrium) was quantified using 1 cm VOIs. Image evaluation was performed using Syngo.via software; Siemens Healthcare [7]. Polar maps of myocardial tracer uptake were created based on the AHA 17-segments model using dedicated software (MunichHeart software, Technical University Munich, Munich, Germany) as previously described [10].

2.5. Statistical analysis

Statistical analyses were performed using GraphPad Prism (version 9.1.0; GraphPad Software, San Diego, California USA). Quantitative values were expressed as mean \pm standard deviation or median and range where appropriate. Comparison of non-parametric data was performed using a Mann-Whitney-U test. All tests were performed two-sided and a p-value < 0.05 was considered to indicate statistical significance.

3. Results

3.1. Patient characteristics

Detailed patient characteristics of the overall cohort are listed in Table 1. The cohort consisted of 11 patients (9/11 males) with AMI as the first manifestation of coronary artery disease (4 patients with NSTEMI and n = 7 patients with STEMI, respectively). Mean age of the patients was 61.0 \pm 8.0 years, with a mean LVEF of 46.7 \pm 12.6 %. One patient had isolated right ventricular AMI. Laboratory parameters of myocardial damage ranged from 852 ng/L to 85295 ng/L for Trop-I_{peak} and 132 U/L to 4562 U/L for peak creatinine kinase (CK). One patient with evidence of ventricular thrombus formation during PET/MRI underwent PET imaging at a second timepoint (470 days after first PET imaging which was 512 days after AMI).

3.2. Image analysis

All patients (11/11, 100 %) showed visually increased myocardial ^{68}Ga -FAPI-46 tracer uptake and clearly definable areas of LGE in the infarcted area. A set of representative images of tracer uptake in STEMI and NSTEMI patients is depicted in Fig. 1. Tracer uptake of infarcted myocardium (SUV_{max}) was significantly higher compared to bloodpool (6.9 \pm 2.3 vs. 2.5 \pm 0.4; p < 0.01) as well as compared to remote myocardium (6.9 \pm 2.3 vs. 2.3 \pm 0.6; p < 0.01), Fig. 2A. SUV_{peak} and

Table 1
Patient characteristics.

Patient characteristics	N = 11
Male sex, n (%)	9 (81.1 %)
Age at AMI, years	61.0 \pm 8.0
LVEF, %	46.7 \pm 12.6
STEMI, n (%)	7 (63.6 %)
NSTEMI, n (%)	4 (36.4 %)
Vessel disease	
3-vessel-disease, n (%)	8 (72.3 %)
2-Vessel-disease, n (%)	1 (9.1 %)
1-Vessel-disease, n (%)	2 (18.2 %)
Median peak Creatine kinase, U/L (Range)	1198.0 (132–4430)
Median peak Myoglobin, $\mu\text{g/L}$ (Range)	218.0 (78–4173)
Median peak Troponin-I, ng/L (Range)	20164.0 (852–84443)
Median peak LDH, U/L (Range)	604.0 (212–1109)
Median peak NT-proBNP, pg/mL (Range)	1265.0 (150–18663)
Days AMI to scan (Median)	30.9 \pm 22.0 (29)

AMI, acute myocardial infarction; LVEF, left ventricular ejection fraction; (N) STEMI, (non)-ST segment myocardial infarction; LDH, lactatdehydrogenase; NT-proBNP, N-terminal pro b-type natriuretic peptide.

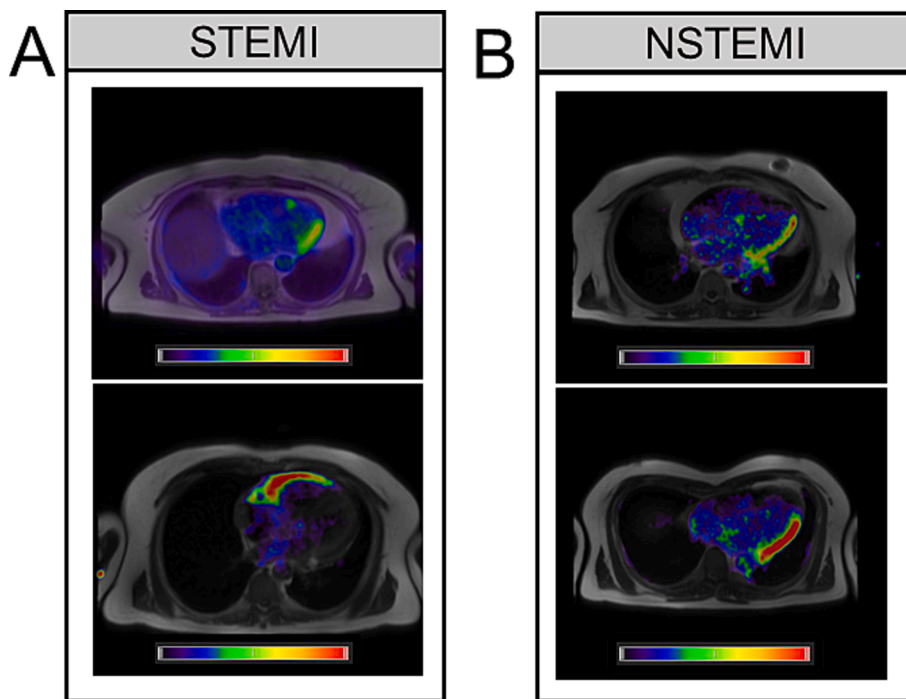


Fig. 1. Representative set of images, showing radiotracer distribution of ⁶⁸Ga-FAPI in axial images of PET/MRI. Tracer uptake shown in two STEMI patients (culprit lesion upper panel: RCX, lower panel: RCA) and two patients after NSTEMI (culprit lesion both panels: RCX); (N)STEMI, (Non)-ST-elevation myocardial infarction; SUV, standard uptake value; RCX, circumflex coronary artery; RCA, right coronary artery.

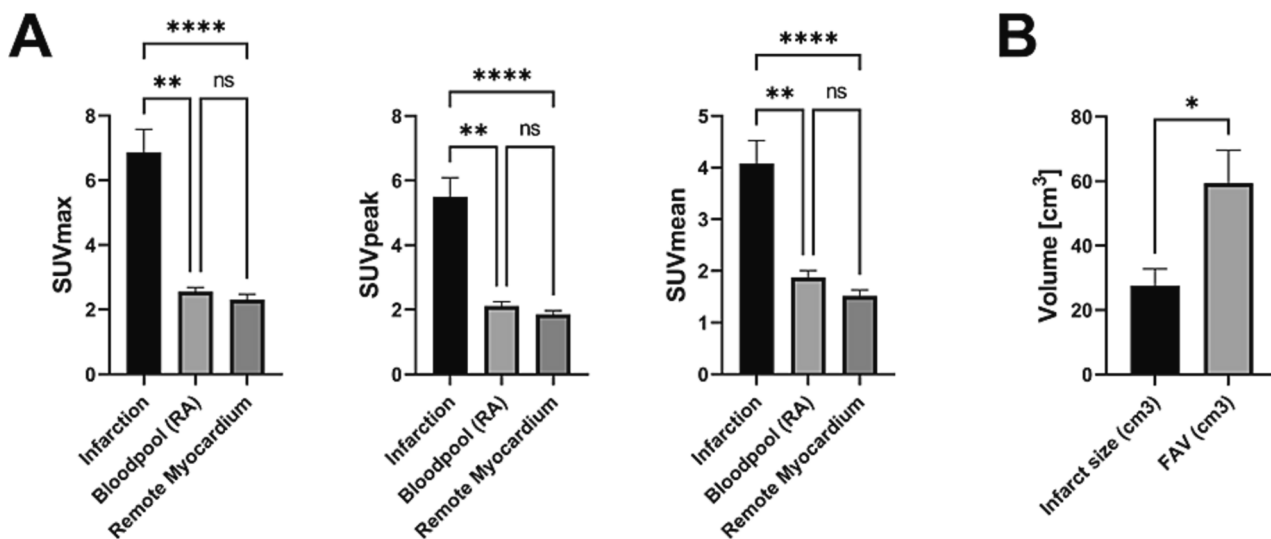


Fig. 2. PET parameter. (A) Uptake parameters for infarcted myocardium (FAV, cm³), bloodpool and remote myocardium. (B) Significant difference between tracer uptake volume (FAV) and volumetric infarct size in magnetic resonance imaging. SUV, standardized uptake value; FAV, fibroblast activation volume; ns, non-significant ($p > 0.05$); * $p < 0.05$, ** $p < 0.01$, **** $p < 0.0001$.

SUV_{mean} showed similar statistically significant results for infarcted myocardium vs. bloodpool and remote myocardium (Fig. 2A). Mean fibroblast activation volume of affected myocardium significantly exceeded the estimated infarct size in MRI estimated by LGE extent (59.5 ± 33.7 vs. 27.6 ± 17.0 cm³; $p < 0.05$, Fig. 2B). In total 57/170 (33.5 %) ⁶⁸Ga-FAPI-46 positive segments were detected compared to 50/170 (29.4 %) segments with positive LGE on MRI.

3.3. Association of ⁶⁸Ga-FAPI-46 PET with MRI and blood biomarkers

Comparison of FAV and MRI infarct size measured by LGE extent

showed a strong correlation ($r = 0.88$; $p < 0.01$). PET tracer uptake intensity showed good correlation with infarct size estimated by LGE (SUV_{max}: $r = 0.68$, $p < 0.05$; SUV_{peak}: $r = 0.74$, $p < 0.05$ and SUV_{mean}: $r = 0.69$, $p < 0.05$). Biomarkers of myocardial damage (lactate dehydrogenase and peak creatinine kinase) showed a strong correlation to infarct size estimated by PET and MR imaging. Details on correlation of PET, MRI parameter and serum biomarkers are depicted in Table 2.

Table 2
Correlation of FAV and MRI infarct size with imaging and biomarkers.

Parameter	Infarct size by FAV (cm ³)		Infarct size by LGE (cm ³)	
	R	P-Value	R	P-Value
FAV			0.88	< 0.01
SUV _{max}	0.55	0.08	0.68	< 0.05
SUV _{peak}	0.62	< 0.05	0.74	< 0.05
SUV _{mean}	0.59	0.06	0.69	< 0.05
Biomarkers				
CK peak	0.67	< 0.05	0.67	< 0.05
CK-MB	0.56	0.10	0.55	0.10
Myoglobin	0.17	0.61	0.35	0.29
Troponin-I	0.61	0.05	0.48	0.14
LDH	0.81	< 0.01	0.82	< 0.01
NT-proBNP	0.47	0.15	0.35	0.29

SUV, standardized uptake value; FAV, fibroblast activation volume; MRI, magnetic resonance imaging; LGE, late gadolinium enhancement; LVEF, left ventricular ejection fraction; CK, creatine kinase, MB, muscle-brain; LDH, lactatdehydrogenase; NT-proBNP, N-terminal pro b-type natriuretic peptide.

3.4. Comparison of STEMI vs. NSTEMI patients with respect to imaging and clinical data

In our sub-analysis of tracer uptake with respect to infarction type, we observed a tendency of higher FAV values (Fig. 3D) in patients after STEMI (64.5 ± 38.4 vs. 50.6 ± 26.1), without reaching statistical significance (p = ns). Other PET parameters were comparable for both cohorts (Fig. 3A-C). This goes in line with the analysis of clinical parameters of myocardial injury confirming no significant difference (both p = ns) between STEMI and NSTEMI patients (CK_{peak} 1387.1 ± 1166.7 and 2292.8 ± 1948.2 U/L; Trop-I_{peak} 32756.9 ± 33282.3 and 41854.5 ± 39828.5 ng/L, for STEMI vs. NSTEMI, respectively).

3.5. Case presentation

A 65 years old male patient after revascularization of an occluded left anterior descending coronary artery was imaged early (42 days) and late (512 days) after AMI with ⁶⁸Ga-FAPI-46 PET/MRI (Fig. 4). Baseline imaging revealed LGE of the apex with thrombus formation in the apical aneurysm and a moderate myocardial tracer uptake. Follow-up imaging revealed persistent tracer uptake and a corresponding scar in the thrombotic aneurysm of the dilated apex. Fibroblast activation volume and infarcted size decreased from baseline to follow-up (FAV: 42.5 to 24.2 cm³; LGE: 31.0 to 22.9 cm³), whereas FAPI-46 uptake intensity remained stable (SUV_{max} 6.3 vs. 6.4; SUV_{mean} 3.9 vs. 4.0; SUV_{peak} 4.8 vs. 5.4). This suggests that although the area of fibroblast activation after AMI is regressing over time, there are remaining areas in the post-ischemic myocardium with ongoing intense fibroblast activation and thus myocardial remodeling processes are detectable even months after infarction.

4. Discussion

This FAPI hybrid PET/MR imaging study was specifically dedicated to visualize fibrotic ventricular remodeling at delayed time points after an ischemic event. Our results confirm that after a mean period of one month following AMI tracer uptake, as surrogate for fibroblast activation, is still present and persistently exceeds the myocardial infarction size as derived from MRI. Further, we report serial FAPI PET imaging in one patient indicating that while the overall extent of fibroblast activation decreases over time, fibroblast activation is present up to 16 months following AMI. This points at the ability of this imaging method to monitor fibrotic remodeling processes in the aftermath of cardiac

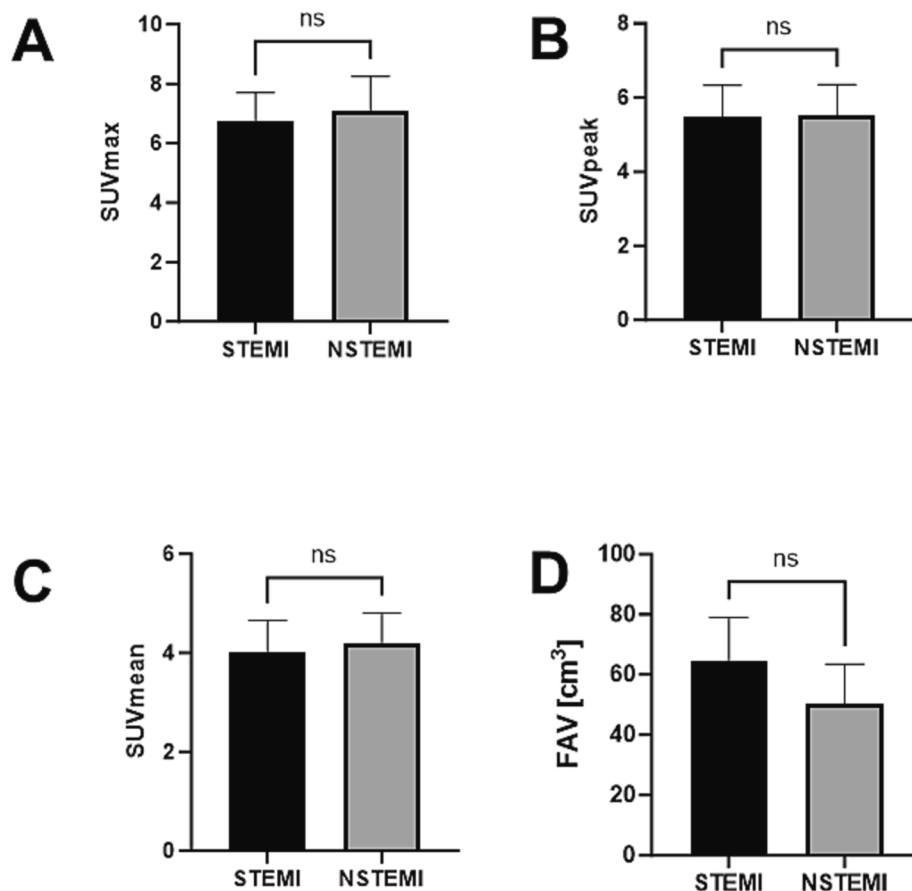


Fig. 3. PET parameters stratified for STEMI and NSTEMI patients showing comparable results, with a tendency of higher FAV values in patients after STEMI. SUV, standardized uptake values; FAV, fibroblast activation volume; (N)STEMI, (non) ST-elevation myocardial infarction.

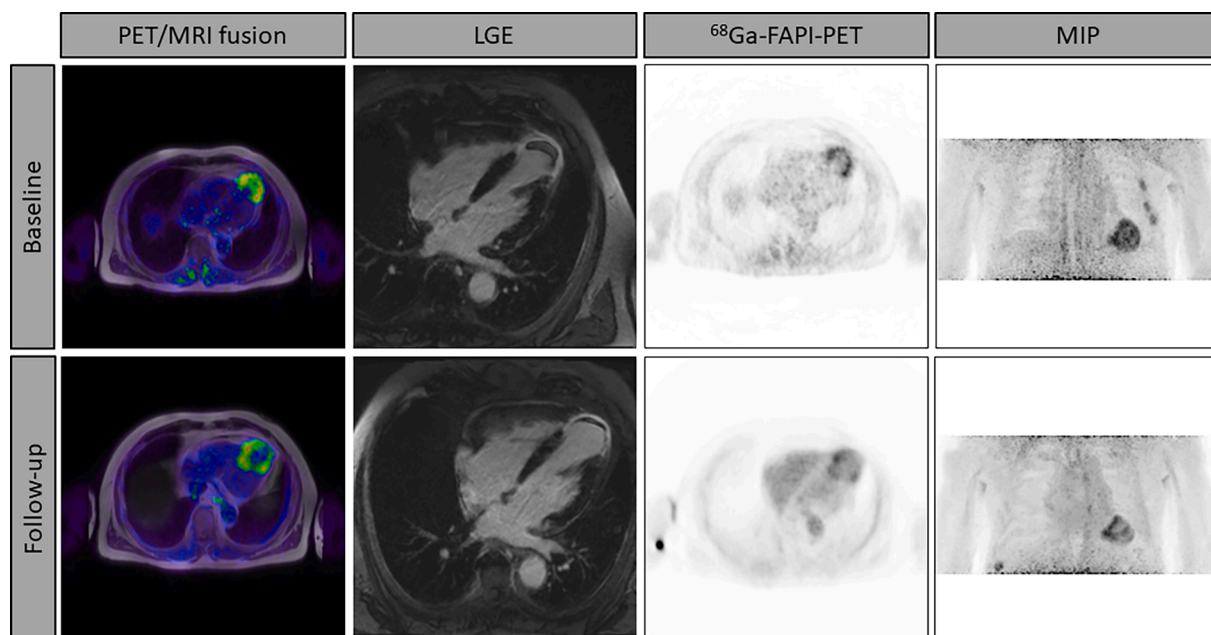


Fig. 4. Repeat FAP imaging in a patient after myocardial infarction. Case example for baseline and follow-up imaging. Baseline images show apical scar with moderate tracer uptake. Follow-up imaging demonstrates the persistence of the scar as well as aneurysmatic apical dilation with corresponding tracer uptake continuing up to 16 months after intervention. PET/MRI, positron-emission tomography/magnetic resonance imaging; FAPI, Fibroblast-Activation Protein-alpha inhibitor; MIP, maximum intensity projection; LGE, left gadolinium enhancement.

injury.

4.1. FAPI findings at a delayed stage after AMI

Our study confirms an increased myocardial tracer uptake as a surrogate for fibroblast activation in infarcted areas compared to remote myocardium and blood pool. The finding of fibroblast activation in the early stages after AMI, which has already been shown in recent analyses, is now complemented with data from delayed PET imaging, with a mean period of 30 days post MI [8,9]. This constitutes an interesting aspect since the timeline of fibrotic remodeling after AMI is still not finally elucidated. Animal models suggest the maximum extent of fibroblast activation within one week after injury [2,9]. It is suggested that this fibroblast activation at an early stage takes place when fibroblasts transform to a pro-inflammatory phenotype and secrete cytokines and chemokines as well as matrix metalloproteinases (MMPs) [11–13]. In the later stages (>30d) fibroblasts are activated to anti-inflammatory and pro-reparative phenotypes and generate anti-inflammatory and pro-angiogenic factors and extracellular matrix components that stabilize the myocardial scar [4,11,14]. The discrepancy between the timeline of fibroblast activation in humans compared to animal models may be explained by the different structures of noncoding ribonucleic acids (RNAs) within the species. The noncoding RNA has been suggested to regulate fibroblast activity in infarcted hearts [15,16]. The overlap of especially long noncoding RNA within mice/humans has been calculated to be only 15 % which is a major limiting factor in the interpretation of studies performed in animal models [1,15–17].

Our delayed imaging approach confirms extensive uptake in this time frame suggesting still major impact of FAP at this stage of remodeling, providing new information for further understanding of timeline and extent of ongoing fibrosis formation, which may shed light on important issues in timing of anti-fibrotic therapies.

4.2. FAPI uptake clearly exceeds myocardial scar as shown by MRI

As suggested by prior studies, LGE is well established for detection of focal replacement fibrosis following ischemic damage [6,18]. However,

LGE does not allow for a differentiation between a fibrosis process that is still in progress and the one that has already been terminated [6,11,19]. Fibroblast activation is a complex interplay between many contributors (tumor necrosis factor alpha, the renin angiotensin aldosterone system) with the timeline of fibrotic remodeling still not finally elucidated [5,20,21]. Fibroblast activation PET imaging offers the chance of a functional assessment of this complex interplay by in-vivo visualization of fibroblast activation. Interestingly at this late stage after AMI, we confirm prior findings that fibroblast activation in affected myocardium still significantly exceeds the infarcted myocardium as delineated by LGE imaging. This supports the hypothesis of fibroblast activation pronounced in the border zone of infarcted myocardium [8]. Further hybrid PET/MRI studies are needed to elucidate the interplay between fibroblast activation, scar formation and adverse left ventricular remodeling. Despite convincing data on imaging of infarcted myocardium, the relevance of fibroblast activation for functional and structural outcome of the affected myocardium is yet to be determined. Our study confirms a strong correlation of standardized tracer uptake parameters with biomarkers of myocardial injury highlighting the impact of FAPI imaging as surrogate of fibroblast activation after myocardial damage in the delayed period after AMI. We were not able to identify differences in FAPI uptake in STEMI vs. NSTEMI patients which can potentially be attributed to the small patient number in this retrospective study.

We present a case with consecutive ^{68}Ga -FAPI-46 PET/MRI scans, in which we report tracer uptake corresponding to the infarcted area that persisted 16 months following AMI, suggesting a long-time frame of tissue remodeling after myocardial injury (Fig. 2).

4.3. Study limitations

We investigated the FAPI imaging in a small cohort with AMI brought on by varying levels of coronary stenoses and different anatomy, which limits the interpretation of statistical relationships between PET parameters, biomarkers and sites and extents of infarction. Another limitation is that most of our patients had multi-vessel coronary artery disease and the degree to which the other non-culprit stenoses have influenced the tracer uptake cannot be determined in this study.

Preliminary data suggest that FAPI uptake might be influenced by various clinical parameters that were not investigated in detail in multivariate models on their influence on tracer uptake due to the limited cohort size. Last, although FAP has been reported a specific biomarker for activated fibroblasts, we cannot rule out FAPI uptake of other cell populations like endothelial cells.

5. Conclusion

In this retrospective study, we demonstrate that ⁶⁸Ga-FAPI-46 PET/MRI is a feasible, hybrid imaging tool for visualization of activated fibroblasts and structural imaging of infarcted myocardium in delayed, subacute stages after AMI. FAPI uptake indicates an interesting biomarker for tissue remodeling, however, an association to a functional outcome has yet to be shown and should be part of future studies. Further studies should provide mechanistic insights in how fibroblasts regulate cardiac remodeling post-AMI and help us understand the mechanistic and temporal process of fibrosis development in order to improve long-term therapies for patients with ischemic heart disease and LV dysfunction. This may have major impact on the pathophysiologic understanding of fibroblast activation after myocardial infarction.

Conflict of interests

W. Fendler reports fees from SOFIE Bioscience (research funding), Janssen (consultant, speaker), Calyx (consultant), Bayer (consultant, speaker, research funding), Parexel (image review), Novartis (speaker), and Telix (speaker) outside of the submitted work. K. Herrmann reports personal fees from Bayer, personal fees and other from Sofie Biosciences, personal fees from SIRTEX, non-financial support from ABX, personal fees from Adacap, personal fees from Curium, personal fees from Endocyte, grants and personal fees from BTG, personal fees from IPSEN, personal fees from Siemens Healthineers, personal fees from GE Healthcare, personal fees from Amgen, personal fees from Novartis, personal fees from ymabs, personal fees from Aktis Oncology, personal fees from Theragnostics, personal fees from Pharma15, personal fees from Debiopharm, personal fees from AstraZeneca, personal fees from Janssen, outside the submitted work.

R. Wakili has received consultant fees, speaking honoraria and travel expenses from Biotronik, Boston Scientific and Medtronic; investigator-initiated funding for research projects (initiated by him) from Bristol-Myers Squibb/Pfizer, and Boston Scientific. R. Wakili was, unrelated to this study, funded by the Deutsche Forschungsgemeinschaft (DFG; German Research Foundation – DO637/23-1; Projektnummer 39443325). C. Rischpler reports a research grant from Pfizer, consultancy for Novartis Radiopharmaceuticals and Pfizer, and speaker honoraria from Alnylam, BTG, Curium, GE Healthcare, Novartis Radiopharmaceuticals, Pfizer, and Siemens Healthineers.

CRediT authorship contribution statement

Jana Kupusovic: Formal analysis, Validation, Writing – original draft, Writing – review & editing. **Lukas Kessler:** Formal analysis, Visualization, Writing – original draft, Writing – review & editing. **Sandra Kazek:** Formal analysis, Validation. **Michal Kamil Chodyla:** Methodology. **Lale Umutlu:** Supervision. **Fadi Zarrad:** Methodology. **Michael Nader:** Methodology. **Wolfgang P. Fendler:** Supervision, Validation. **Zohreh Varasteh:** Methodology, Writing – review & editing. **Ken Hermann:** Supervision. **Dobromir Dobrev:** Supervision, Writing – original draft. **Reza Wakili:** Supervision, Validation. **Tienush Rassaf:** Supervision. **Johannes Siebermair:** Conceptualization, Data curation, Formal analysis, Investigation, Methodology, Supervision,

Validation, Writing – original draft, Writing – review & editing. **Christoph Rischpler:** Conceptualization, Investigation, Methodology, Supervision, Validation, Writing – original draft, Writing – review & editing.

Declaration of competing interest

The authors declare that they have no known competing financial interests or personal relationships that could have appeared to influence the work reported in this paper.

References

- [1] C. Humeres, N.G. Frangogiannis, Fibroblasts in the infarcted, remodeling, and failing heart, *JACC Basic Transl. Sci.* 4 (3) (2019) 449–467.
- [2] J. Tillmanns, D. Hoffmann, Y. Habbaba, J.D. Schmitto, D. Sedding, D. Fraccarollo, P. Galuppo, J. Bauersachs, Fibroblast activation protein alpha expression identifies activated fibroblasts after myocardial infarction, *J. Mol. Cell Cardiol.* 87 (2015) 194–203.
- [3] T. Lindner, A. Loktev, A. Altmann, F. Giesel, C. Kratochwil, J. Debus, D. Jäger, W. Mier, U. Haberkorn, Development of quinoline-based theranostic ligands for the targeting of fibroblast activation protein, *J. Nucl. Med.* 59 (9) (2018) 1415–1422.
- [4] M.G. Sutton, N. Sharpe, Left ventricular remodeling after myocardial infarction: pathophysiology and therapy, *Circulation* 101 (25) (2000) 2981–2988.
- [5] S. Nattel, Molecular and CELLULAR MECHANISMS OF ATRIAL FIBROSIS IN ATRIAL FIBRILLATION, *JACC Clin. Electrophysiol.* 3 (5) (2017) 425–435.
- [6] S. Ørn, C. Manhenke, I.S. Anand, I. Squire, E. Nagel, T. Edvardsen, K. Dickstein, Effect of left ventricular scar size, location, and transmural extent on left ventricular remodeling with healed myocardial infarction, *Am. J. Cardiol.* 99 (8) (2007) 1109–1114.
- [7] L. Kessler, J. Kupusovic, J. Ferdinandus, N. Hirmas, L. Umutlu, F. Zarrad, M. Nader, W.P. Fendler, M. Totzeck, R. Wakili, T. Schlosser, T. Rassaf, C. Rischpler, J. Siebermair, Visualization of fibroblast activation after myocardial infarction using ⁶⁸Ga-FAPI PET, *Clin. Nucl. Med.* 46 (10) (2021) 807–813.
- [8] J. Diekmann, T. Koenig, J.T. Thackeray, T. Derlin, C. Czerner, J. Neuser, T.L. Ross, A. Schäfer, J. Tillmanns, J. Bauersachs, F.M. Bengel, Cardiac fibroblast activation in patients early after acute myocardial infarction: integration with MR tissue characterization and subsequent functional outcome, *J. Nucl. Med.* 63 (9) (2022) 1415–1423.
- [9] Z. Varasteh, S. Mohanta, S. Robu, M. Braeuer, Y. Li, N. Omidvari, G. Topping, T. Sun, S.G. Nekolla, A. Richter, C. Weber, A. Habenicht, U.A. Haberkorn, W. A. Weber, Molecular imaging of fibroblast activation after myocardial infarction using a (⁶⁸Ga)-labeled fibroblast activation protein inhibitor, FAPI-04, *J Nucl Med* 60 (12) (2019) 1743–1749.
- [10] S.G. Nekolla, C. Miethaner, N. Nguyen, S.I. Ziegler, M. Schwaiger, Reproducibility of polar map generation and assessment of defect severity and extent assessment in myocardial perfusion imaging using positron emission tomography, *Eur. J. Nucl. Med.* 25 (9) (1998) 1313–1321.
- [11] Y. Ma, R.P. Iyer, M. Jung, M.P. Czubryt, M.L. Lindsey, Cardiac fibroblast activation post-myocardial infarction: current knowledge gaps, *Trends Pharmacol. Sci.* 38 (5) (2017) 448–458.
- [12] A.V. Shinde, N.G. Frangogiannis, Fibroblasts in myocardial infarction: a role in inflammation and repair, *J. Mol. Cell Cardiol.* 70 (2014) 74–82.
- [13] D. Bací, A. Bosí, L. Parisi, G. Buono, L. Mortara, G. Ambrosio, A. Bruno, Innate immunity effector cells as inflammatory drivers of cardiac fibrosis, *Int. J. Mol. Sci.* 21 (19) (2020) 7165.
- [14] E.A. Rog-Zielinska, R.A. Norris, P. Kohl, R. Markwald, The living scar-cardiac fibroblasts and the injured heart, *Trends Mol. Med.* 22 (2) (2016) 99–114.
- [15] E.E. Creemers, E. van Rooij, Function and therapeutic potential of noncoding RNAs in cardiac fibrosis, *Circ. Res.* 118 (1) (2016) 108–118.
- [16] T. Thum, Noncoding RNAs and myocardial fibrosis, *Nat. Rev. Cardiol.* 11 (11) (2014) 655–663.
- [17] V.R. Paralkar, T. Mishra, J. Luan, Y.u. Yao, A.V. Kossenkov, S.M. Anderson, M. Dunagin, M. Pimkin, M. Gore, D. Sun, N. Konuthula, A. Raj, X. An, N. Mohandas, D.M. Bodine, R.C. Hardison, M.J. Weiss, Lineage and species-specific long noncoding RNAs during erythro-megakaryocytic development, *Blood* 123 (12) (2014) 1927–1937.
- [18] E.B. Schelbert, et al., Late gadolinium-enhancement cardiac magnetic resonance identifies postinfarction myocardial fibrosis and the border zone at the near cellular level in ex vivo rat heart, *Circ. Cardiovasc. Imaging* 3 (6) (2010) 743–752.
- [19] S. Notohamiprodjo, et al., Imaging of cardiac fibroblast activation in a patient after acute myocardial infarction using ⁶⁸Ga-FAPI-04, *J. Nucl. Cardiol.* 29 (5) (2022) 2254–2261.
- [20] F.G. Spinale, Myocardial matrix remodeling and the matrix metalloproteinases: influence on cardiac form and function, *Physiol. Rev.* 87 (4) (2007) 1285–1342.
- [21] T. Liu, et al., Current understanding of the pathophysiology of myocardial fibrosis and its quantitative assessment in heart failure, *Front. Physiol.* 8 (2017) 238.